



HAL
open science

Tracking quasi-classical chaos in ultracold boson gases

Maxence Lepers, Véronique Zehnlé, Jean Claude Garreau

► **To cite this version:**

Maxence Lepers, Véronique Zehnlé, Jean Claude Garreau. Tracking quasi-classical chaos in ultracold boson gases. *Physical Review Letters*, 2008, 101 (14), pp.144103. 10.1103/PhysRevLett.101.144103 . hal-00309094

HAL Id: hal-00309094

<https://hal.science/hal-00309094>

Submitted on 5 Aug 2008

HAL is a multi-disciplinary open access archive for the deposit and dissemination of scientific research documents, whether they are published or not. The documents may come from teaching and research institutions in France or abroad, or from public or private research centers.

L'archive ouverte pluridisciplinaire **HAL**, est destinée au dépôt et à la diffusion de documents scientifiques de niveau recherche, publiés ou non, émanant des établissements d'enseignement et de recherche français ou étrangers, des laboratoires publics ou privés.

Tracking quasi-classical chaos in ultracold boson gases

Maxence Lepers, Véronique Zehnlé, and Jean Claude Garreau

Laboratoire de Physique des Lasers, Atomes et Molécules,

*Université des Sciences et Technologies de Lille; CNRS; F-59655 Villeneuve d'Ascq Cedex**

We study the dynamics of a ultra-cold boson gas in a lattice submitted to a constant force. We track the route of the system towards chaos created by the many-body-induced nonlinearity and show that relevant information can be extracted from an experimentally accessible quantity, the gas mean position. The threshold nonlinearity for the appearance of chaotic behavior is deduced from KAM arguments and agrees with the value obtained by calculating the associated Lyapunov exponent.

PACS numbers: 03.75.Nt, 05.45.Ac, 37.10.Jk

Recent advances in the physics of cold atoms paved the way for the investigation of fundamental quantum problems with unprecedented cleanness. “Quantum chaos” is one of the most fascinating among these problems, because in such case the correspondence between the dynamics of the quantum system and its classical counterpart is nontrivial. The reasons for that are twofold: First, quantum particles obey Heisenberg inequalities, hence their dynamics cannot be described in terms of phase-space trajectories. Second, sensitivity to initial conditions is not observed, as the Schrödinger equation is linear. For these reasons, *quantum chaos* has often been defined as “the behavior of a quantum system whose classical limit is chaotic”. Whereas this is a reasonable definition, it is clear that the actual quantum dynamics has no direct relation to classical chaos. Much work thus concentrates in finding “reminiscences” of classical chaos that might survive in the quantum system, the so-called “signatures” of quantum chaos [1].

The realization in 1995 of the first Bose-Einstein condensate with laser-cooled atoms [2, 3, 4] opened a new way for investigating (truly) nonlinear dynamics in quantum systems. In an “ideal” (i.e. in the zero temperature limit) Bose-Einstein condensate (BEC), the atoms are indistinguishable and form a mesoscopic object which can be described by a “collective” single wavefunction. The BEC’s dynamical behavior is then described by the Gross-Pitaevskii equation which includes a *nonlinear* term due to atomic interactions [5]. The solutions of such equation can – and do – present sensitivity to initial conditions, leading to “classical-like” instabilities, a possibility that attracted much attention from both theoreticians [6, 7, 8, 9, 10, 11, 12, 13, 14] and experimentalists [15, 16].

In order to make these ideas clear, let us first consider a simpler system, the kicked rotor, whose experimental realization with laser cooled atoms [17] lead to an impressive burst of experimental work [18, 19, 20, 21, 22, 23, 24, 25]. This system is formed by a particle periodically “kicked” by a sinusoidal force. The classical dynamics is characterized by a single parameter K , which is the normalized amplitude of the potential [17], whereas the

“quanticity” of the quantum system is described by a “normalized Planck constant” \hbar (the dynamics become classical as $\hbar \rightarrow 0$).

In order to characterize the dynamics, one may chose, for instance, the particle’s square momentum as the relevant quantity ($p^2(t)$ in the classical case, $\langle p^2(t) \rangle$ in the quantum case). By taking the Fourier transform of the above quantity and pinpointing the frequencies appearing in the evolution of the system for different values of K and fixed initial conditions, we can characterize in a common language the classical and the quantum versions. The result is plotted in Fig. 1.

The classical dynamics, Fig. 1a, shows resonances (or frequency-lock events) each time a frequency become very close to another one. For $K \gtrsim 0.8$, the frequencies in the spectrum “coalesce” to form of a dense spectrum, which is a signature of a chaotic dynamics. In the quantum case, Fig. 1b, the spectrum is richer and present numerous frequency crossings, but no dense spectrum is observed.

Let us now consider a one-dimensional BEC of particles of mass M placed in a sinusoidal lattice formed by counterpropagating laser beams of wavelength λ_L , and subjected to a linear force. The system is described by the Gross-Pitaevskii equation (GPE)

$$i\frac{\partial\psi(x,t)}{\partial t} = \left(\frac{P^2}{2m} + V_0 \cos(2\pi x) + Fx + g|\psi|^2 \right) \psi(x,t), \quad (1)$$

with lengths measured in units of the lattice step $d = \lambda_L/2$, energy measured in units of the recoil energy $E_R = \hbar^2 k_L^2 / (2M)$ (with $k_L = 2\pi/\lambda_L$), time in units of \hbar/E_R , the force F in units of E_r/d , $P = -i\partial/\partial x$, the reduced mass is $m = \pi^2/2$ and g is the (1D) nonlinear parameter. The eigenstates of the linear part of the Hamiltonian (1), obtained by setting $g = 0$, are the so-called Wannier-Stark (WS) states [6, 26, 27]. In order to simplify the discussion, let us we suppose that the BEC energy is low enough that its wavefunction ψ can be expanded only on the lowest-energy WS state for each potential well, hereafter noted as $\varphi_n(x)$ (corresponding to the n^{th} well). These states are centered at each potential well, obey the symmetry relation $\varphi_{n+m}(x) = \varphi_n(x - m)$, and form a

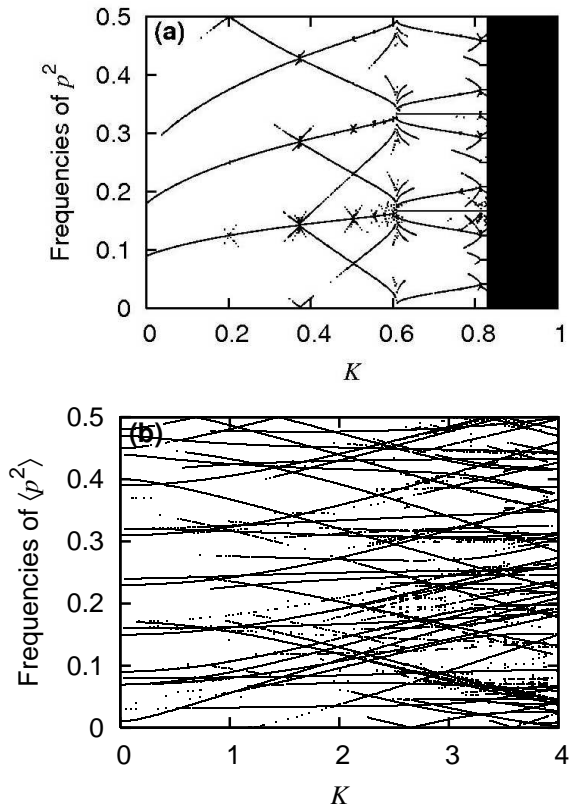


Figure 1: Classical and quantum dynamics of the kicked rotor. For each value of K , we numerically calculate $p^2(t)$ (classical case) and $\langle p^2(t) \rangle$ (quantum case) up to 2000 kicks, perform the Fourier transform and pinpoint the frequencies whose Fourier amplitude is above a threshold (here $1/500$ of the maximum amplitude). (a) Frequencies in the classical dynamics: A dense spectrum appears for $K \gtrsim 0.82$ (initial conditions $x = 0$ and $p = 0.56$). (b) Frequencies in the quantum dynamics: The spectrum is complex, but always discrete ($\bar{k} = 2.89$, the initial state is a Gaussian in momentum space of FWHM $5\bar{k}$ centered at $p = 0.56$).

ladder of eigenenergies $E_n = n\omega_B$, where $\omega_B = Fd/\hbar$ (F in our normalized units) is the Bloch frequency. Thus, putting $\varphi(x) \equiv \varphi_0(x)$

$$\psi(x, t) = \sum_n \sqrt{I_n} e^{-i\theta_n} \varphi(x - n), \quad (2)$$

where the eigenstates population I_n and phase θ_n are real functions of the time.

Following the approach of [6], we insert Eq. (2) in Eq. (1), and obtain Hamilton equations for the populations and phases. The Hamiltonian then appears as a sum of an integrable part H_0 and a non-integrable perturbation H_1 :

$$H = H_0(I) + \epsilon H_1(I, \theta), \quad (3)$$

with $\epsilon \propto g\chi_{01}$, where $\chi_{0i} \equiv \int dx \varphi^3(x) \varphi(x - i)$ is a measure of the superposition of eigenfunctions correspond-

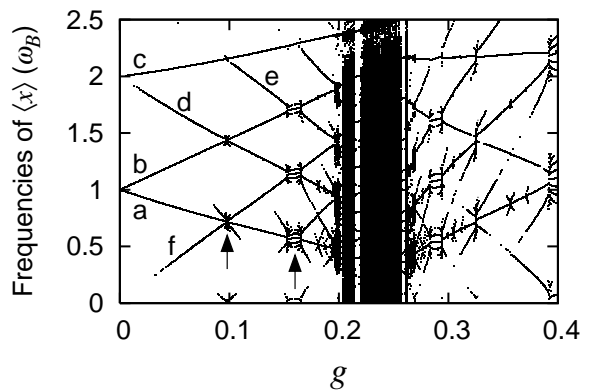


Figure 2: Frequencies present in the spectrum of $\langle x(t) \rangle$ vs g (the threshold is $1/100$ of the maximum amplitude). For small g , the Bohr frequencies [cf. Eq. (4)] are $\omega_{10} = \omega_B - 0.4g\chi_{00}$, $\omega_{0-1} = \omega_B + 0.55g\chi_{00}$ and $\omega_{1-1} = 2\omega_B + 0.15g\chi_{00}$, corresponding to branches a, b, and c, respectively. Harmonics of ω_{10} are also seen (branches d and e) and $\Omega_{1,-1,0}$ (branch f). For $0.22 \lesssim g \lesssim 0.26$ one observes dense-spectrum windows corresponding to quasi-classical chaos. Parameters are $\omega_B = 0.25$, $V = 5$ ($\chi_{00} = 2$); initial conditions are $I_0 = 0.65$, $I_1 = 0.25$, $\theta_0 = \theta_{-1} = 0$, $\theta_1 = \pi$.

ing to different wells. For small ϵ , the system is quasi-integrable and fits into the general frame of the KAM theorem [28]. Therefore, the quantum-coherent evolution of a BEC displays classical-like KAM-structured chaos. We call this, “quasi-classical” chaos.

If we temporarily neglect the nonlinear term in Eq. (1), we see that the phases evolve as $\theta_n(t) = \theta_{n0} + n\omega_B t$. To the first order in ϵ , the effect of the nonlinearity is to introduce a population-dependent correction to this phase, producing a harmonic evolution with frequencies $\omega_n = n\omega_B + g\chi_{00}I_n$. The intensities are constants of motion, $I_n(t) = I_n(t = 0)$ and the “self-coupling” parameter χ_{00} depends only V_0 and F . The BEC dynamics is thus governed by the Bohr frequencies

$$\omega_{nm} \equiv \omega_n - \omega_m = (n - m)\omega_B + g\chi_{00}(I_n - I_m). \quad (4)$$

In order to simplify further our description, let us restrict the dynamics to three adjacent potential wells, i.e. we set $I_n \equiv 0$ if $n \neq -1, 0, 1$ in Eq. (2). The system is then four-dimensional, the dynamical variables being two populations (since $I_{-1} + I_0 + I_1 = 1$) and two relative phases.

The onset of chaos in this system is shown in Fig. 2, which is the equivalent of Fig. 1 for the BEC dynamics, with the difference that we used the average position $\langle x(t) \rangle$ instead of $\langle p^2(t) \rangle$. Strikingly, the plot resembles more closely to the *classical* (Fig. 1a) than to the quantum (Fig. 1b) dynamics of the kicked rotor.

We can interpret the main features of Fig. 2 from simple arguments. At $g = 0$ there are only three Bohr frequencies in the model: Two of them are degenerated,

$\omega_{0-1} = \omega_{10} = \omega_B$, and correspond to energy difference between neighbor wells, whereas $\omega_{-11} = 2\omega_B$ corresponds to next-to-neighbor energy difference. The low- g structure can be understood using Eq. (4). The frequencies present around $g = 0.05$, for instance, in Fig. 2 are of the form

$$\Omega_{pqr} = p\omega_{0-1} + q\omega_{10} + r\omega_{-1} \quad (5)$$

with p, q, r integer. Namely, from top to bottom, we found ω_{1-1} , $2\omega_{10}$, ω_{0-1} , ω_{10} and $\omega_{0-1} - \omega_{10}$. These frequencies are only weakly perturbed by the nonlinearity, which manifests itself by the slight curvature of the branches. A KAM-type expansion in powers of ϵ shows that the weight of a frequency Ω_{pqr} in the spectrum is proportional to g/Ω_{pqr} [28], thus, the higher the value of g , the larger the number of frequencies that will be present (remember that Fig. 2 displays the frequencies whose amplitude is above a threshold), and smaller frequencies will be favored. The intersection of two branches correspond to a resonance, that is, the condition $\Omega_{pqr} = 0$ is fulfilled for some p, q, r . Close to a resonance the KAM perturbation theory breaks down, and non-integrable behaviors appear that may lead to chaos. In Fig. 2 the arrows indicate the resonances $\Omega_{1q0} = 0$ ($q = -2$) for $g \approx 0.093$, and $q = -3, -4, -5$ for, respectively, $g \approx 0.14$, $g = 0.17$, $g = 0.196$. For higher g values, resonances with higher and higher q values become significative, as seen on the left of the chaotic region: Each frequency crossing produces a multi-frequency structure (indicated by the arrows). Finally, for $g \gtrsim 0.2$ one observes at least four successive windows of dense spectrum, corresponding to a chaotic behavior.

Fig. 2 represents a “local route” (in the sense that its detailed geometry depends on the initial conditions) to quasi-classical chaos. The above argument suggests however that this route is characteristic of KAM systems, and globally independent of initial conditions. Its universal character is confirmed by comparing it to Fig. 1a, where an analogous structure is observed in a completely different KAM system, the classical kicked rotor. We have thus put into evidence a route to KAM chaos in a nonlinear quantum system, which is potentially observable with state-of-art experiments.

In order to confirm our conclusions, we have also calculated the maximum Lyapunov exponent (MLE) associated to the dynamics, which is a direct signature of the sensitivity to the initial conditions, and thus of chaos. In order to calculate MLEs in our quantum system, we adapted the classical Jacobian method [29]. We represent the system evolution by a trajectory in a six-dimensional “generalized quantum phase-space”, formed by the real and imaginary parts of each WS state coefficient, i.e. $\sqrt{I_n} \cos \theta_n$ and $\sqrt{I_n} \sin \theta_n$, for $n = -1, 0, 1$ (this is numerically more stable than using I_n and θ_n), and calculate the divergence of neighbor WS states, from which we can extract the MLE. The result is presented in

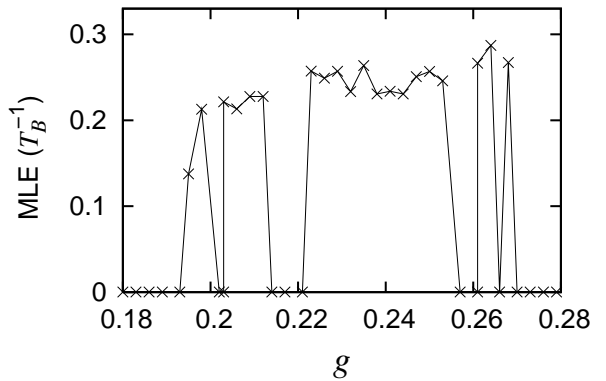


Figure 3: Maximum Lyapunov exponent (in units of $T_B^{-1} = \omega_B/2\pi$) as a function of g . One observes a good correspondence between the existence of a non-zero Lyapunov exponent and the presence of dense-spectrum regions in Fig. 2. The observed dense-spectrum is thus a reliable signature of the chaotic behavior. Same parameters and initial conditions as in Fig. 2.

Fig. 3. One sees a clear transition to chaos for $g \approx 0.194$, which is in good agreement with the value that can be deduced from Fig. 2. We can also identify the four successive chaotic windows.

For given initial conditions, we can obtain an estimate for the critical value of g at which chaos appears. KAM theory shows that chaos generally appears along a separatrix. In our system there are two main kinds of trajectories [6]: “Passing” trajectories correspond to Bloch oscillations slightly perturbed by the nonlinearity (for the low values of g we are considering); they appear when the three populations are comparable. Bound, periodic orbits correspond to a motion essentially confined at a potential well, and appear when one population dominates the others. Between these two kinds of trajectories, there is a separatrix. For a given trajectory (i.e. for fixed initial conditions), chaos appears when the changing in the value of g brings it close to the separatrix. The condition for that can be simply estimated by confining the BEC to only two wells ($I_{-1} = 0$), in which case the system is integrable. This “reduced” system does not exhibit chaos, but it has a phase-space structure analogous to that of the 3-wells, displaying bound and passing trajectories, and, between them, a separatrix. In the reduced system we can calculate both the energy E_0 corresponding to the trajectory (with $I_{-1} = 0$) and the energy E_s of the unstable point to which the separatrix is connected. We can then numerically determine the value of g for which $E_0 = E_s$, which gives the critical value. Fig. 4 shows the result for various initial conditions (solid line). The dotted lines indicate the limits of the chaotic region as inferred from the Lyapunov exponent calculation in the 3-well system. The agreement is very good, even when

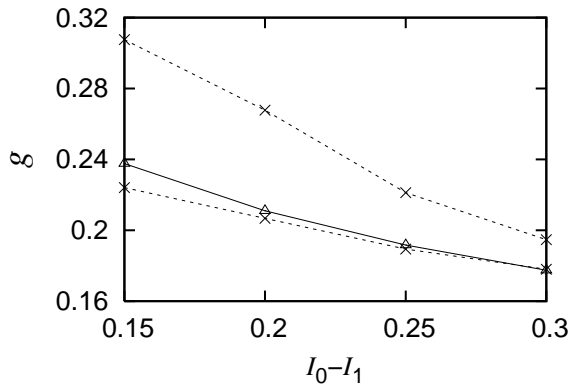


Figure 4: Determination of the critical value of g . The solid lines with triangles are the estimated critical value of g , given by the condition that the trajectory energy equals the separatrix energy (cf. text). The dotted lines with crosses are the limits of the chaotic region, where the Lyapunov exponent is non-zero. The parameters are the same as in Fig 2, with $\theta_0 - \theta_1 = \frac{\pi}{2}$.

the chaotic zone is narrow.

In conclusion, we have characterized the phenomenon of quasi-classical chaos using an experimentally accessible signal, the mean position of the boson gas. We have studied a “local route” to quasi-classical chaos and shown that the information obtained from this approach agrees well with that provided by a hallmark signature of chaos, the sensitivity to initial conditions, quantified by a positive Lyapunov exponent. The understanding of the structure of such a route allowed us to determine the critical value of the nonlinearity parameter, which is in good agreement with the one deduced from the calculation of the Lyapunov exponent. We think that the present work might stimulate an experimental observation of quasi-classical chaos, which would, in turn, stimulate new investigations on the nature of quantum chaos.

The authors are happy to thank M. Lefranc for fruitful discussions and for his help with the calculation of Lyapunov exponents.

* URL: <http://phlam.univ-lille1.fr/atfr/cq>

- [1] F. Haake, *Quantum Signatures of Chaos* (Springer-Verlag, Berlin, Germany, 2001), 2nd ed.
 [2] M. H. Anderson, J. R. Ensher, M. R. Matthews, C. E. Wieman, and E. A. Cornell, *Science* **269**, 198 (1995).
 [3] C. C. Bradley, C. A. Sackett, J. J. Tollett, and R. G. Hulet, *Phys. Rev. Lett.* **75**, 1687 (1995).

- [4] W. Ketterle, *Rev. Mod. Phys.* **74**, 1131 (2002).
 [5] F. Dalfovo, S. Giorgini, L. Pitaevskii, and S. Stringari, *Rev. Mod. Phys.* **71**, 463 (1999).
 [6] Q. Thommen, J. C. Garreau, and V. Zehnlé, *Phys. Rev. Lett.* **91**, 210405 (2003).
 [7] Y. Zheng, M. Koštrun, and J. Javanainen, *Phys. Rev. Lett.* **93**, 230401 (2004).
 [8] G. P. Berman, F. Borgonovi, F. M. Izrailev, and A. Smerzi, *Phys. Rev. Lett.* **92**, 030404 (2004).
 [9] J. Fang and W. Hai, *Physica B* **370**, 61 (2005).
 [10] D. Witthaut, M. Werder, S. Mossmann, and H. J. Korsch, *Phys. Rev. E* **71**, 036625 (2005).
 [11] J. Liu, C. Zhang, M. G. Raizen, and Q. Niu, *Phys. Rev. A* **73**, 013601 (2006).
 [12] S. Wimberger, P. Schlagheck, and R. Mannella, *J. Phys. B: At. Mol. Opt. Phys.* **39**, 729 (2006).
 [13] N. van Noort, M. A. Porter, Y. Yi, and S. N. Chow, *J. Nonlinear Sci.* **17**, 59 (2007).
 [14] J. Reslen, C. E. Creffield, and T. S. Monteiro, *Phys. Rev. A* **77**, 043621 (2008).
 [15] L. Fallani, L. De Sarlo, J. E. Lye, M. Modugno, R. Saers, C. Fort, and M. Inguscio, *Phys. Rev. Lett.* **93**, 140406 (2004).
 [16] M. Christiani, O. Morsch, N. Malossi, M. Jona-Lasinio, M. Anderlini, E. Courtade, and E. Arimondo, *Opt. Exp.* **12**, 4 (2004).
 [17] F. L. Moore, J. C. Robinson, C. F. Bharucha, B. Sundaram, and M. G. Raizen, *Phys. Rev. Lett.* **75**, 4598 (1995).
 [18] H. Ammann, R. Gray, I. Shvachuck, and N. Christensen, *Phys. Rev. Lett.* **80**, 4111 (1998).
 [19] M. K. Oberthaler, R. M. Godun, M. B. d’Arcy, G. S. Sully, and K. Burnett, *Phys. Rev. Lett.* **83**, 4447 (1999).
 [20] L. Deng, E. W. Hagley, J. Denschlag, J. E. Simsarian, M. Edwards, C. W. Clark, K. Helmerson, S. L. Rolston, and W. D. Phillips, *Phys. Rev. Lett.* **83**, 5407 (1999).
 [21] J. Ringot, P. Szriftgiser, J. C. Garreau, and D. Delande, *Phys. Rev. Lett.* **85**, 2741 (2000).
 [22] P. Szriftgiser, J. Ringot, D. Delande, and J. C. Garreau, *Phys. Rev. Lett.* **89**, 224101 (2002).
 [23] G. J. Duffy, S. Parkins, T. Müller, M. Sadgrove, R. Leonhardt, and A. C. Wilson, *Phys. Rev. E* **70**, 056206 (2004).
 [24] H. Lignier, J. Chabé, D. Delande, J. C. Garreau, and P. Szriftgiser, *Phys. Rev. Lett.* **95**, 234101 (2005).
 [25] C. E. Creffield, G. Hur, and T. S. Monteiro, *Phys. Rev. Lett.* **96**, 024103 (2006).
 [26] G. H. Wannier, *Phys. Rev.* **117**, 432 (1960).
 [27] Q. Thommen, J. C. Garreau, and V. Zehnlé, *Phys. Rev. A* **65**, 053406 (2002).
 [28] A. J. Lichtenberg and M. A. Leiberman, *Regular and Chaotic Dynamics* (Springer-Verlag, Berlin, Germany, 1982).
 [29] J. P. Eckmann and D. Ruelle, *Int. J. Mod. Phys.* **57**, 617 (1985).